

Conf. 9/12/53

# THEORETICAL DESCRIPTION OF ELECTROMAGNETIC PION PRODUCTION

T.-S. H. Lee  
Argonne National Laboratory  
Argonne, IL 60439-4843 USA

ANL/CP--75001

DE92 005222

## ABSTRACT

Theoretical models for describing electromagnetic production of pions are reviewed. Recent results of  $N(\gamma, \pi)$ ,  $N(e, e' \pi)$  and  $d(e, e' \pi)$  calculated from a Hamiltonian model are presented.

Extensive work on the electromagnetic production of pions on the nucleon has been carried out since the publication of the pioneering work by Chew, Goldberger, Low and Nambu<sup>1</sup> (CGLN). In this talk I will first give a brief review of the main theoretical approaches developed in the last 34 years, and then discuss a recently constructed Hamiltonian model which can be applied to investigate all aspects of physics that is to be discussed at this conference.

Basically there exist three main approaches. The first one is the extension of the CGLN model based on the dispersion-relation formulation. The dispersion-relation approach was subsequently applied by Fubini, Nambu and Wataghlin<sup>2</sup> to study electroproduction of pions. It makes use of the properties of unitarity, analyticity and crossing symmetry to express the photoproduction amplitudes in terms of  $\pi N$  scattering amplitudes and the Born terms calculated from a Lagrangian. Schematically, the fixed-t dispersion relation for the photoproduction amplitude is of the following form

**MASTER**

**DISTRIBUTION OF THIS DOCUMENT IS UNLIMITED**

### DISCLAIMER

*ps*

This report was prepared as an account of work sponsored by an agency of the United States Government. Neither the United States Government nor any agency thereof, nor any of their employees, makes any warranty, express or implied, or assumes any legal liability or responsibility for the accuracy, completeness, or usefulness of any information, apparatus, product, or process disclosed, or represents that its use would not infringe privately owned rights. Reference herein to any specific commercial product, process, or service by trade name, trademark, manufacturer, or otherwise does not necessarily constitute or imply its endorsement, recommendation, or favoring by the United States Government or any agency thereof. The views and opinions of authors expressed herein do not necessarily state or reflect those of the United States Government or any agency thereof.

The submitted manuscript has been authored by a contractor of the U. S. Government under contract No. W-31-109-ENG-38. Accordingly, the U. S. Government retains a nonexclusive, royalty-free license to publish or reproduce the published form of this contribution, or allow others to do so, for U. S. Government purposes.

$$\text{Re}A_i(s, t) = A_i^{\text{Born}}(s, t) + \frac{P}{\pi} \int_{(m+\mu)^2}^{\infty} ds' \left[ \frac{1}{s'-s} + \frac{1}{s'-u} \right] \text{Im}A_i(s', t) \quad (1)$$

where  $s$ ,  $t$  and  $u$  are the familiar Mandelstam variables, and  $A^{\text{Born}}$  can be calculated from the usual pseudoscalar coupling Born terms. In the static cutoff Chew-Low model, the partial-wave solution  $M_{\ell\pm}$  of Eq. (1) was found in Ref. 1

$$M_{\ell\pm} = \frac{M_{\ell\pm}^{\text{Born}}}{f_{\ell\pm}^{\text{Born}}} f_{\ell\pm}$$

where  $f_{\ell\pm}$  is the  $\pi N$  partial-wave amplitude. It is, however, a very difficult numerical task to find the general solution of the dispersion relation Eq. (1), mainly because it is a singular integral equation and no solution exist unless some fall-off behavior of the amplitude at large  $s$  is assumed. One also has to assume that the multipole expansion of all invariant amplitudes is convergent outside the physical region ( $|\cos(\cos\theta)| > 1$ ) at all energies. This is certainly not true for the amplitudes  $A_2$  and  $A_5$ . Nevertheless, numerical methods were developed and the solutions for describing the data up to the  $\Delta$  energy region were found, as reviewed by Donnachie<sup>3</sup>. It is however not clear how to interpret the multipole amplitudes obtained from these earlier works, since the assumptions that were made could be inconsistent with the modern theory of strong interactions. It is an interesting question to explore in the future.

The second approach is the effective Lagrangian method which utilizes Chiral symmetry. By gauging an effective Lagrangian to include coupling to the electromagnetic field, the pion photoproduction mechanism is calculated with perturbation theory in the tree-approximation (only keeping the terms without loop integrations). The final  $\pi N$  interaction is accounted for by using

Watson's theorem. This requires that the phase of each photoproduction multipole amplitude is identical to the  $\pi N$  scattering phase in the same eigenchannel. This approach was thoroughly investigated by Olsson and Osypowski<sup>4</sup>. They emphasized that the pion photoproduction mechanism should be calculated with pseudovector coupling, as required by Chiral symmetry. They also found that a satisfactory agreement with data can only be achieved when the exchange of vector mesons, and an explicit treatment of the  $\Delta$  degree of freedom are included. Their approach was further developed by Wittman, Mukhopadhyay and Davidson<sup>5</sup>, as well as by Sabutis<sup>6</sup>. The model developed by Blomquist and Laget<sup>7</sup> can be considered as a variation of the effective Lagrangian approach.

Here it is necessary to point out that in the two approaches described above, the final  $\pi N$  interaction is described only by the  $\pi N$  scattering phase shifts. Within their theoretical frameworks, no procedure is defined to calculate the off-shell amplitudes which are indispensable in nuclear calculations. Clearly we have to go beyond these two approaches in order to study electromagnetic production of pions on nuclei, which will be the focus of future experiments.

We now turn to describe the third approach. It is a Hamiltonian formulation which is closely related to two recent developments in intermediate energy nuclear physics: (1) the construction of a nuclear Hamiltonian with  $\pi, N$  and  $\Delta$  degrees of freedom - especially as arising in the extensive studies of the  $\pi NN$  system<sup>8</sup>, (2) the study of nucleon structure and  $\pi N$  scattering within the chiral bag model<sup>9</sup> or its variations. It is assumed that the  $\pi N$  interaction Hamiltonian consists of a  $\pi N \leftrightarrow N, \Delta$  vertex and a  $\pi N$  potential. The electromagnetic parts of the Hamiltonian are defined in terms of matrix elements calculated from a Lagrangian using perturbation theory. The first attempts to construct such a Hamiltonian model were made by Tanabe and Ohta<sup>10</sup>, who considered only the  $\pi N P_{33}$  channel, and independently by Yang<sup>11</sup>,

who considered all s- and p-wave amplitudes. These two works concentrate on the determination of magnetic M1 and electric E2 transition strengths of the  $\Delta$  excitation. The extent to which the experimental observables can be described by these two models is not reported. The most ambitious attempt is the one developed by Araki and Afnan<sup>12</sup>. They employed the diagrammatic method to derive a set of coupled  $\pi N$ - $\gamma N$  unitary equations from the cloudy bag Lagrangian. No numerical results based on their approach have been reported so far.

In a collaboration with Nozawa and Blankleider, we have taken the third approach to construct<sup>13,14</sup> a Hamiltonian model which is aimed at achieving the following goals: (1) it is unitary and gauge invariant, (2) it can describe most of the existing data of  $\gamma N \leftrightarrow \pi N$  and  $N(e,e'\pi)N$  reactions below the  $2\pi$ -production threshold, (3) it accounts for the magnetic M1, electric E2 and charge form factors of  $\Delta \leftrightarrow \gamma N$  excitation, while at the same time being consistent with the current understanding of hadron structure, (4) it can be straightforwardly used in investigating intermediate energy electromagnetic interactions with two- and many-nucleon systems. In the past two years, the model has been improved in several directions. In the remainder of this talk I will describe the main ingredients of the model and then report on the status of the model and its application in the study of  $(e,e'\pi)$  reaction on deuteron and heavier nuclei.

We started with an effective Lagrangian describing interactions among fields of the nucleon, delta, pion, rho, and omega mesons. The form of the interaction Lagrangian is constrained only by various well-established symmetry properties of  $\pi N$  and  $\gamma N$  reactions. Among them, chiral symmetry is the most important one if the threshold properties of  $\pi N$  and  $\gamma N$  interaction can be described in the tree-diagram approximation. Our interest is, however, not limited in the energy region near the threshold. We want to describe all data from the threshold up to the  $\Delta$  excitation energy

region. It is therefore necessary to go beyond the lowest order tree-diagram approximation. Historically, such attempts have been made to study  $\pi\pi$  and  $\pi N$  scattering. It was found that the number of phenomenological parameters needed to regularize the loop integrations and to describe the data increases as the considered energy increases. Furthermore, the resulting amplitudes are too cumbersome for nuclear calculations. The situation is similar in the recent chiral perturbation theory calculation.

The Hamiltonian formulation can be considered as an alternative to these higher order calculations based on an effective Lagrangian. The main advantage is that it is consistent with the existing nuclear models and hence can be directly applied for nuclear calculations.

Starting from an effective Lagrangian, it is straightforward to calculate the lowest order Feynman amplitudes for the photoproduction of a  $\pi N$  state from a nucleon. In a Hamiltonian approach, one simply assumes that these amplitudes with all hadronic external legs put on their mass shell are the lowest order terms in a perturbation expansion of the scattering amplitude defined by a Hamiltonian of the following form

$$H = H_S + \int [J_{\text{Born}}^\mu(x) + J_\Delta^\mu(x)] A_\mu(x) dx \quad (2)$$

where  $A_\mu$  is the electromagnetic field,  $J_\mu^\mu$  are current operators. The hadronic interactions are defined by

$$H_S = H_0 + H'_S \quad (3)$$

with

$$H'_S = \sum_{B=N,\Delta} f_{\pi N,B} + v_{\pi N,\pi N} \quad (4)$$

where  $H_0$  is the sum of free energy operators for  $\pi$ ,  $N$  and  $\Delta$ ,  $f_{\pi N,B}$  is a  $\pi N \leftrightarrow B$  vertex interaction, and  $v_{\pi N,\pi N}$  is a nonresonant  $\pi N$  potential.

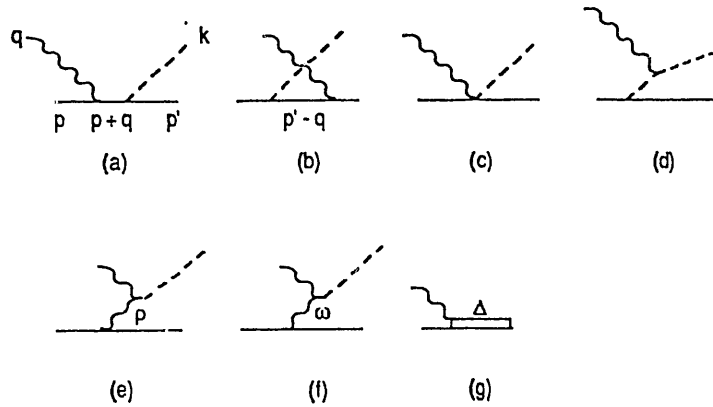


Fig. 1. Photoproduction mechanisms.

The current operators are defined by the Feynman amplitudes given in Fig. 1. Amplitudes of Fig. 1(a)-(f) are traditionally called the "Born terms". The matrix elements of the nonresonant current operator of Eq. (2) are defined by

$$\langle \vec{k}, \vec{p}' | J_{\text{Born}}^{\mu}(0) | \vec{p} \rangle = \left[ \frac{\Lambda^2}{\Lambda^2 + \vec{k}^2} \right] \times [\text{Born terms}]_{(a)-(f)} \quad (5)$$

where  $\vec{k}$  is the  $\pi N$  relative momentum and  $\Lambda$  is a cut-off parameter. The form factor in Eq. (5) is introduced to assure that the current operator is integratable. All parameters of the nonresonant terms (Fig. 1(a)-(f)) are taken from the literature.

The  $\Delta$  current is defined by Fig. 1(g). Its matrix element can be written as

$$\langle \vec{p}_{\Delta} | J_{\Delta}^{\mu}(0) | \vec{p} \rangle = \bar{w}^{\mu}(p_{\Delta}) \Gamma_{\mu\nu} u(p) \quad (6)$$

when  $w^{\mu}(p_{\Delta})$  is the Rarita-Schwinger spinor. We follow Jones and Scadron<sup>16</sup> to define the  $\gamma N \leftrightarrow \Delta$  vertex as

$$\Gamma_{\mu\nu} = G_M(q^2) K_{\mu\nu}^M + G_E(q^2) K_{\mu\nu}^E + G_C(q^2) K_{\mu\nu}^C. \quad (7)$$

Note that the form factors  $G_M(q^2)$ ,  $G_E(q^2)$  and  $G_C(q^2)$  in Eq. (7) are bare form factors which get dressed by pions in the presence of the hadronic interaction  $H_S$  defined in Eq. (2). The kinematic factors  $K_{\mu\nu}$  in Eq. (7) are given in Ref. 15.

We mention here that the current matrix elements defined above involve complicated momentum-dependences which are expected to be essential in understanding the data at high energies. We retain all of these features in our formulation of the problem. No nonrelativistic expansion of these matrix elements is made.

With the dynamics defined by Eqs. (2)-(4), the photoproduction amplitude is of the following form

$$T_{\pi N, \gamma N}(kp', qp) = \langle \chi_{\vec{k}, \vec{p}}^{(-)} | J_{\text{Born}}^\mu(0) + J_\Delta^\mu(0) | p \rangle \epsilon_\mu(q, \lambda) \quad (8)$$

where  $\epsilon_\mu$  is the photon polarization vectors and  $\chi^{(-)}$  is the  $\pi N$  scattering state. It is determined from the hadronic Hamiltonian

$$\langle \chi_{\vec{k}, \vec{p}}^{(-)} | = \langle \vec{k} \vec{p} | [1 + T_{\pi N, \pi N}(E) \frac{1}{E_0 - H + i\epsilon}] \quad (9)$$

where  $T_{\pi N, \pi N}$  is the  $\pi N$  scattering operator defined by

$$T_{\pi N, \pi N}(E) = H'_S + H'_S \frac{1}{E - H_S + i\epsilon} H'_S \quad (10)$$

Explicitly, we have in the center of mass frame

$$\begin{aligned} & \langle \chi_{\vec{k}}^{(-)} | J_{\text{Born}}^\mu(0) | \vec{p} \rangle \\ &= \langle \vec{k} | J_{\text{Born}}^\mu(0) | \vec{p} \rangle + \int d\vec{k}' T_{\pi N, \pi N}(\vec{k}, \vec{k}', E) \frac{\langle \vec{k}' | J_{\text{Born}}^\mu(0) | \vec{p} \rangle}{E - E_{\vec{k}'} - E_{\vec{k}'} + i\epsilon} \end{aligned} \quad (11.a)$$

$$\langle \chi_{\vec{k}}^{(-)} | J_\Delta^\mu(0) | \vec{p} \rangle = \tilde{f}_{\pi N, \Delta}(\vec{k}) \frac{1}{E - m_{0\Delta} - \Sigma_\Delta(E)} \langle \vec{p}_\Delta | J_\Delta^\mu(0) | \vec{p} \rangle \quad (11.b)$$

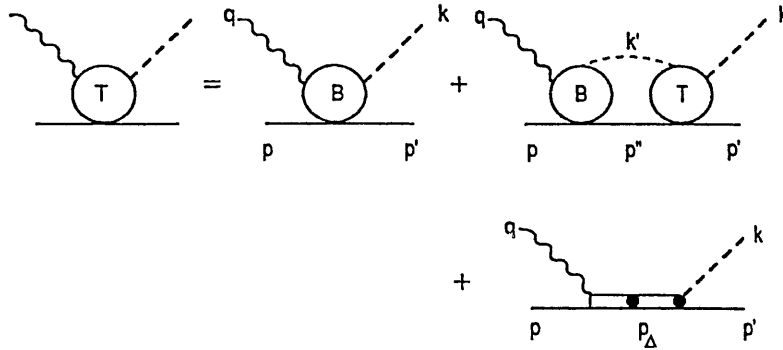


Fig. 2. Graphical representation of Eq. (11).

where  $E$  is the total c.m. energy,  $m_{\Delta}$  is the bar mass of the  $\Delta$ ,  $\Sigma_{\Delta}$  is the  $\Delta$  self-energy, and  $\mathcal{T}_{\pi N, \Delta}$  is the dressed  $\pi N \leftrightarrow \Delta$  vertex. Both  $\Sigma_{\Delta}$  and  $\mathcal{T}_{\pi N, \Delta}$  are calculated from the interaction  $H_S^1$ . Equation (11) is represented diagrammatically in Fig. 2.

The gauge invariance requires that the current matrix elements satisfy the following current conservation condition

$$\langle \chi_{\vec{k}, \vec{p}'}^{(-)} | j_{\mu}(0) | \vec{p} \rangle q = 0 . \quad (12)$$

In a Hamiltonian formulation, the above condition does not follow automatically from the dynamics defined by Eqs. (2)-(11). This originates from that the current matrix elements involved in the integration of Eq. (11) can be off-energy-shell ( $E \neq E_N(\vec{\kappa}') + E_{\pi}(\vec{\kappa}')$ ), and hence there is an arbitrariness in defining the time component of the intermediate state in calculating Eq. (5) from each diagram in Fig. 1. For example, the time component of the intermediate nucleon of Fig. 1(a) could be  $p_0'' = q_0 + E_N(\vec{p})$  or  $E_{\pi}(\vec{k}) + E_N(\vec{p}')$ . The choice has to be made such that Eq. (12) is satisfied. We have found that this can be easily achieved by equating the intermediate momenta to the sum of the external



momenta according to the momentum conservation at the photon vertex; i.e.  $p_0 = q_0 + E_N(\vec{p})$  for Fig 1(a). The details have been given explicitly in Refs. 13 and 14. In the model of Yang, he uses the kinematics which will occur in the application of the model in two-nucleon calculations to define a procedure. The gauge invariance condition was not addressed by Tanabe and Ohta<sup>10</sup>.

We now turn to describe how the model is constructed in practice. The first step of course is to determine the hadronic Hamiltonian  $H'_S$ . This is done by carrying out the fits to the  $\pi N$  phase shifts. The second step is then to adjust the cutoff  $\Lambda$  and the strengths of  $\gamma N \leftrightarrow \Delta$  vertex functions  $G_M(0)$ ,  $G_E(0)$  to get the best description of "all" observables of  $\gamma N + \pi N$  reactions, or the deduced multipole amplitudes. The  $q^2$ -dependence of form factors are then determined from the study of  $N(e, e' \pi)$  processes. The determination of these form factors are in fact the main goal, since they contain the information of the structure of  $N$  and  $\Delta$ . We emphasize here that this cannot be achieved in a simple approach just using the Watson theorem to treat the involved  $\pi N$  dynamics.

For simplicity, separable forms of  $v_{\pi N, \pi N}$  are assumed in all earlier work<sup>10-14</sup>. This is of course theoretically very unsatisfactory, since  $v_{\pi N, \pi N}$  plays an important role in determining the off-shell behavior of the  $\pi N$   $t$ -matrix in the second term of Eq. (11.a). This term is called the final-state-interaction (FSI). The importance of using a correct off-shell  $t$ -matrix was first emphasized by Yang. For example, the threshold of  $E_{0+}$  amplitudes of the  $\gamma p + \pi^0 p$  reaction can vary from -1.92 to +0.64 by using different separable  $v_{\pi N, \pi N}$  models, which are phase-shift equivalent in the low-energy region. The focus of our effort in the last two years is to construct a meson-exchange  $\pi N$  model from an effective Lagrangian. The procedure is to find a three-dimensional reduction to derive the scattering Eq. (10) from the  $\pi N$  Bethe-Salpeter equation. This is being done in a collaboration with Yang's group at Taiwan National University. At the present time, we<sup>16</sup> are able to get a good fit to

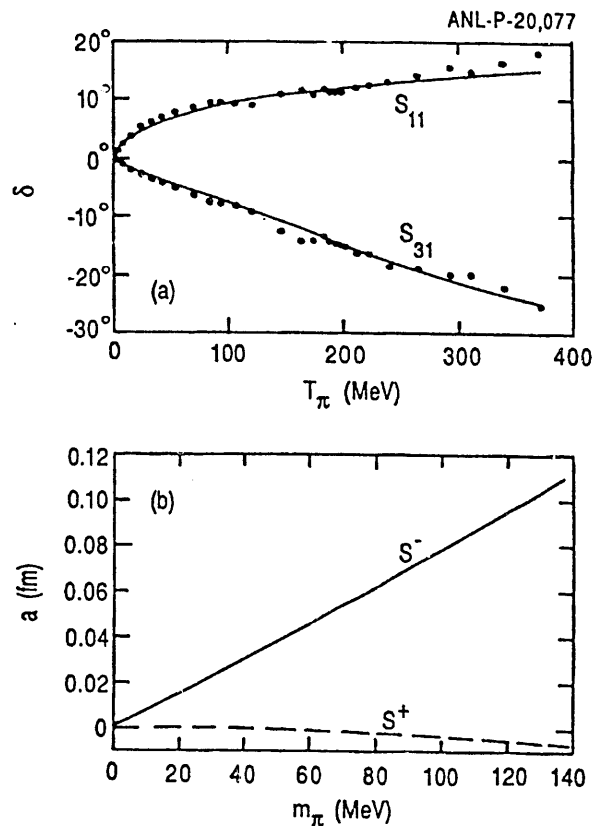


Fig. 3. The  $\pi N$  s-wave scattering results from the Pearce-Jenning  $\pi N$  model.  $\delta$  is the  $\pi N$  phase shift and  $s^\pm = a_{3/2} \pm a_{1/2}$  are the combinations of two s-wave scattering lengths.

the  $\pi N$   $S_{11}$ ,  $S_{31}$  and  $P_{33}$  phase shifts. But the fits to the other p-waves are only very qualitative. In a separate collaboration with Pearce and Nozawa, we<sup>17</sup> have succeeded in casting the meson-exchange  $\pi N$  model of Pearce and Jenning<sup>18</sup> into a form consistent with Eq. (10). An important feature of the Pearce-Jenning model is that it has the correct chiral limit, which is illustrated in Fig. 3. As the pion mass approaches zero, the chiral limit of the s-wave scattering lengths  $s_+ + s_- \rightarrow 0$  is obtained. At higher energies, the FSI calculated from this meson-exchange model is very different from our previous calculation using separable  $v_{\pi N, \pi N}$ . The best fit to all differential cross sections of  $\gamma N \rightarrow \pi N$  are achieved by setting  $\Lambda = 550$  MeV,  $G_M(0) = 3.065$  and  $G_E(0) = 0.07$ . These are

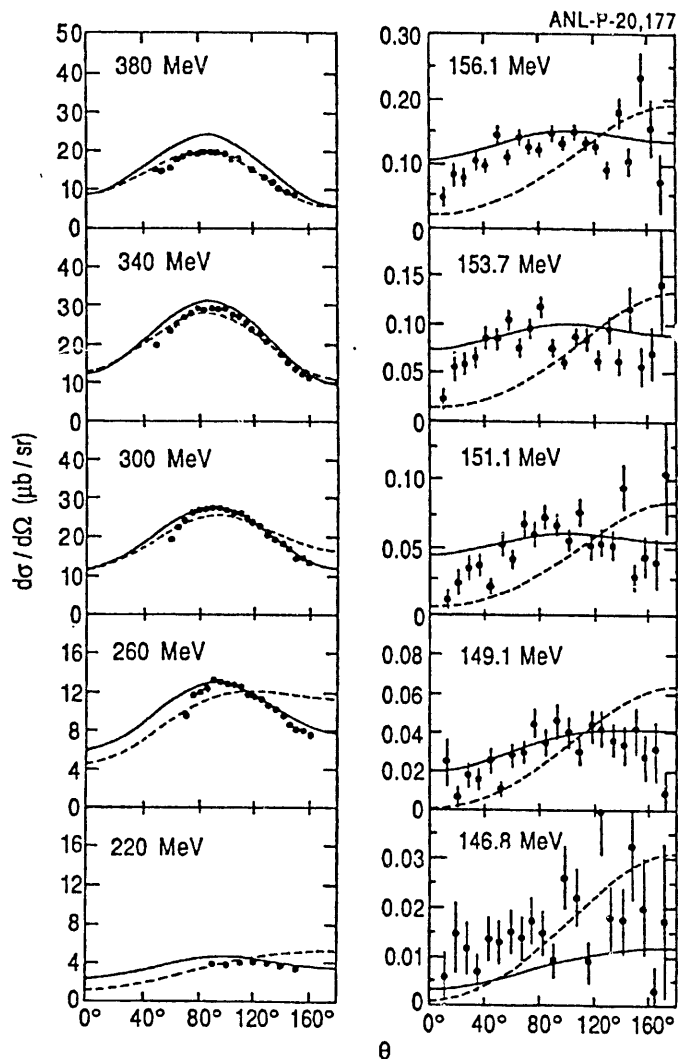


Fig. 4. The differential cross section of  $\gamma p \rightarrow \pi^0 p$  for using the meson-exchange  $\pi N$  model (solid curves) and separable  $\pi N$  model (dashed).

significantly different from the values  $\Lambda = 600$  MeV,  $G_M(0) = 2.28$  and  $G_E(0) = 0.07$  determined in our earlier work<sup>13,14</sup> using the separable  $\pi N$  model. In general, two calculations give an equally good description of the differential cross section of charged pion production. The main difference is that the meson-exchange model gives a significantly better account of the data of  $\gamma p \rightarrow \pi^0 p$  processes, as illustrated in Fig. 4. Note that the results in the low-

energy regions  $E_\pi \leq 156.17$  eV are scaled by a factor of 0.8 and hence our meson-exchange calculations do not give a quantitative account of the data near the threshold. It is, however, interesting to note that our  $E_{O^+}$  amplitudes (Fig. 5) are not too different from that deduced from the Mainz data. The structure near 152 MeV is due to the cusp effect. It can be calculated naturally in our Hamiltonian approach, as discussed in detail in Ref. 19. I will not further discuss pion photoproduction near the threshold. This will be discussed by the next speaker. I only want to point out that we now have concluded that because of the approximations, such as the use of a three-dimensional reduction, involved in constructing the Hamiltonian model from a chiral invariant Lagrangian, our approach cannot be used to explore the interesting question concerning the low-energy theorem. We are more interested in obtaining a model which can account for very intensive data from the threshold up to the  $\Delta$  region. It then can be used to explore nuclear dynamics.

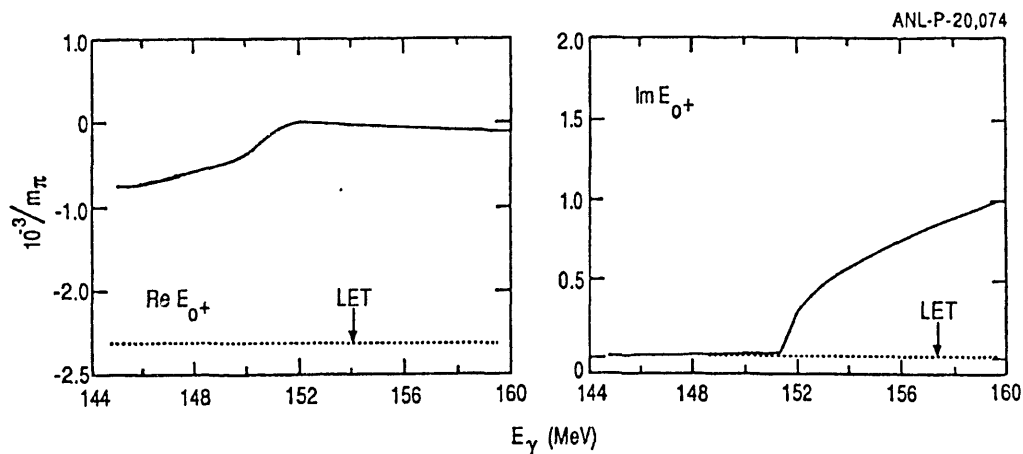


Fig. 5. The  $E_{O^+}$  amplitude of  $\gamma p \rightarrow \pi^0 p$  calculated in Ref. 17.

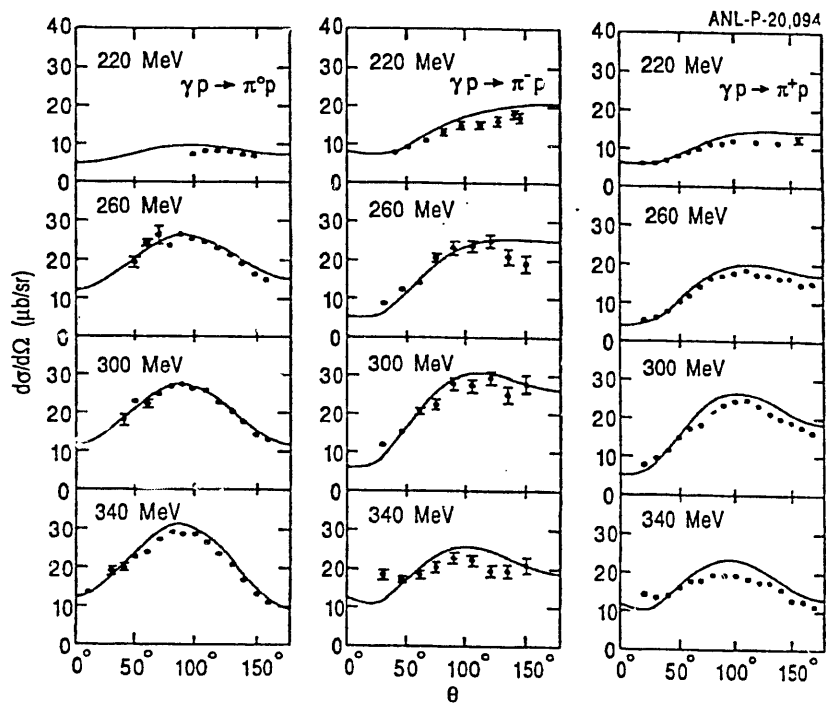


Fig. 6. Differential cross sections of  $\gamma N \rightarrow \pi N$  calculated in Ref. 17.

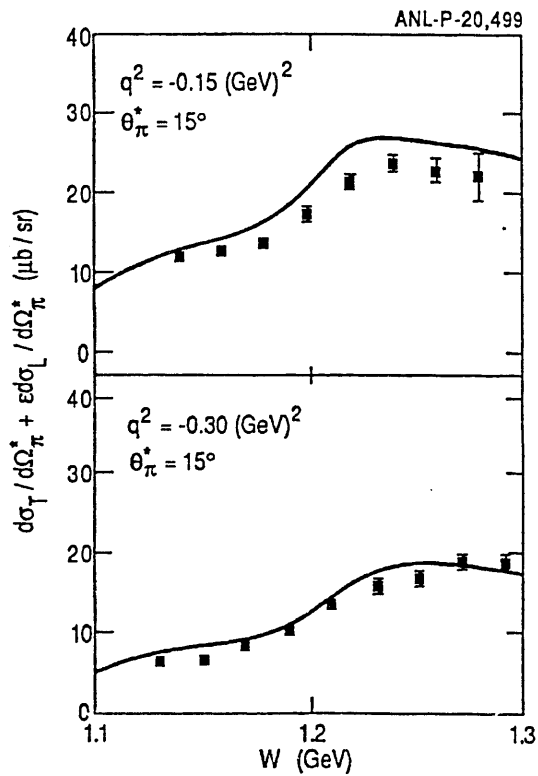


Fig. 7. Results of  $N(e, e' \pi)$  cross section from Ref. 14.

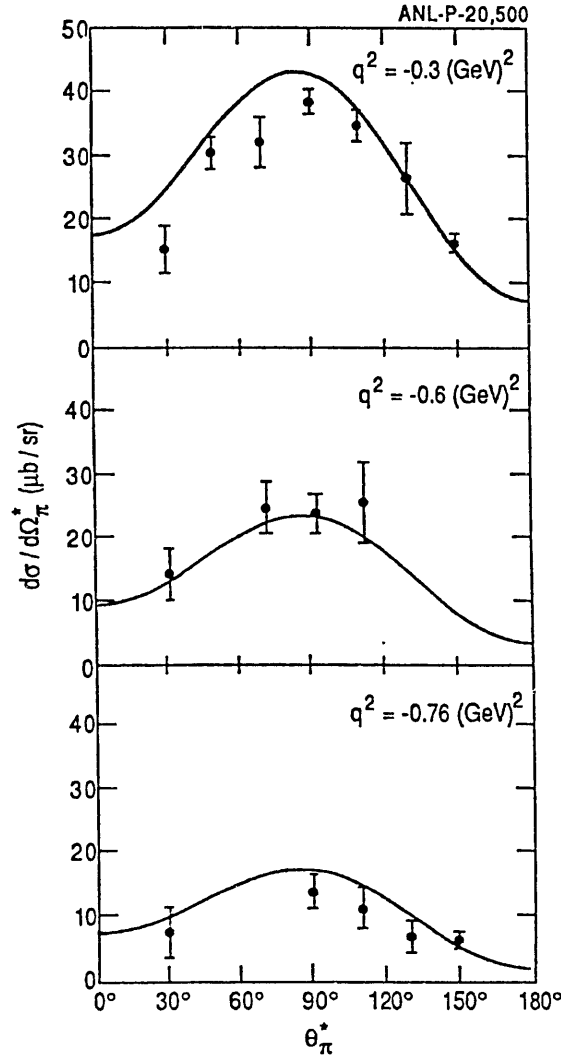


Fig. 8. Results of  $N(e,e'\pi)$  cross section from Ref. 14.

In Figs. 6-9, we display some selected results from our extensive calculations published in Refs. 13, 14 and 17. We see that our model can give a good account of the existing data. An important feature of our approach is the calculation of the FSI from the off-shell  $\pi N$  t-matrix. This is illustrated in Fig. 10. We see that a very large part of the calculated cross section is from the FSI term. This further indicates the importance of developing a theoretically-sound  $\pi N$  model.

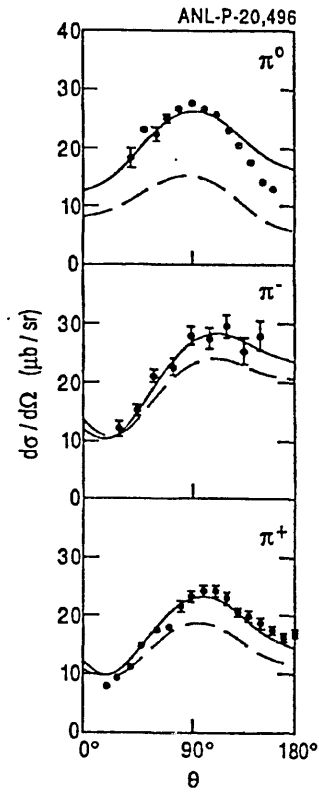


Fig. 9. Results of  $\gamma N \rightarrow \pi N$  cross section from Ref. 14. The dashed curve is from calculations by setting the FSI term to zero.

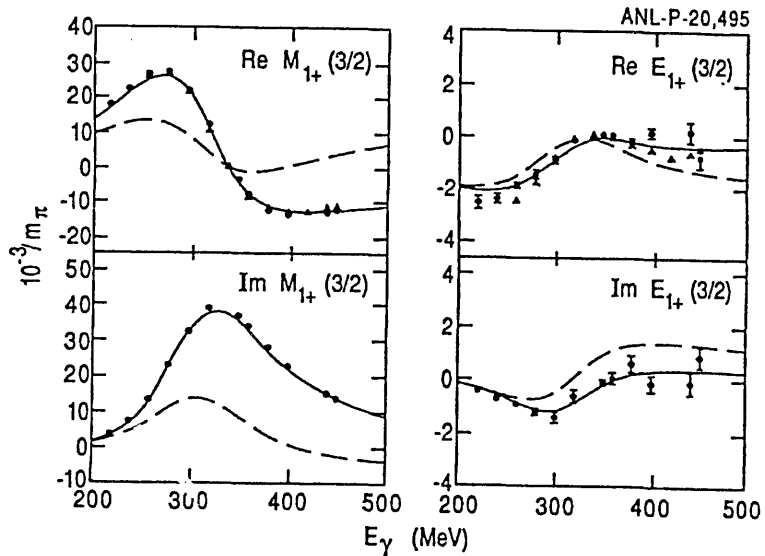


Fig. 10. Results of multipole amplitudes from Ref. 14. The dashed curve is when the  $\Delta$ -term is set to zero.

In Fig. 11, we show the fit to amplitudes in the  $P_{33}$   $\Delta$ -excitation channel. The dashed curves are from the Born term Eq. (11.a) which is sensitive to the choice of  $v_{\pi N, \pi N}$ . The fits (solid curves) are obtained by adjusting  $G_M(0)$  and  $G_E(0)$  of Eq. (7). The large difference between the solid and dashed curves explains why the values of  $G_M(0)$  and  $G_E(0)$  determined from our recent meson-exchange calculation are significantly different from our earlier results. We emphasize that only when the meaning of the dynamical content of  $v_{\pi N, \pi N}$  is well defined, such as the meson-exchange model, the physical meaning of the extracted forms of  $G_M(0)$  and  $G_E(0)$  can be interpreted.

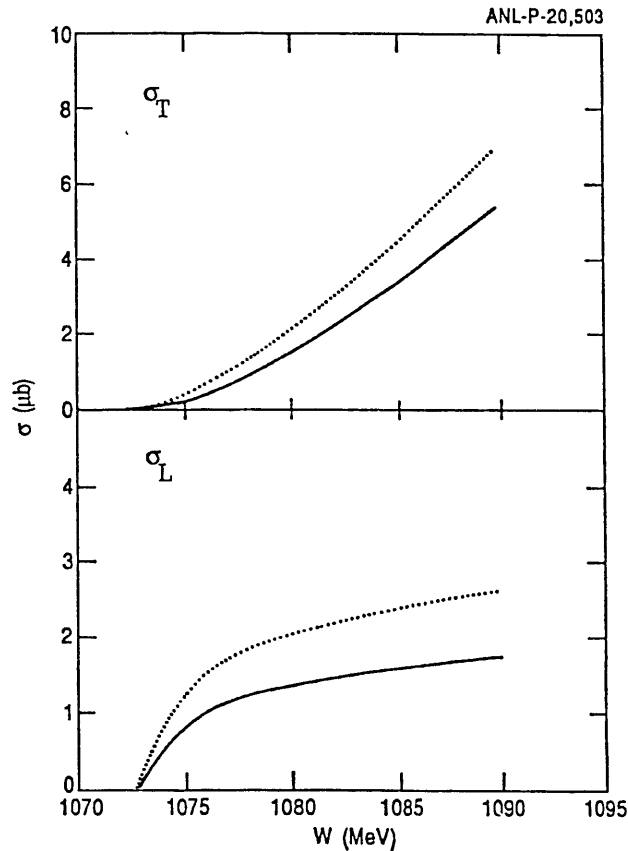


Fig. 11. The total longitudinal ( $\sigma_t$ ) and transverse ( $\sigma_L$ ) cross section of  $p(e, e' \pi^0)$ . The solid (dotted) curves are for  $q^2 = 0.05$  ( $-0.1$ )  $(\text{GeV}/c)^2$ ,  $W = 1075$  MeV and  $\epsilon = 0.82$ .



Further work with Pearce and Nozawa is underway to pin down the forms of  $G_M(q^2)$ ,  $G_E(q^2)$  and  $G_C(q^2)$  by carrying out extensive calculations of various spin observables of both the photo- and electroproduction of pions. Our results will be published in the near future.

In Fig. 12, we show our prediction of  $p(e,e'\pi^0)$  for the NIKHEF kinematics. It is seen that it has a strong  $q^2$ -dependence. Comparison with the data will be interesting. In Fig. 13, we compare our recent calculations of  $p(e,e'\pi)$  with the data from

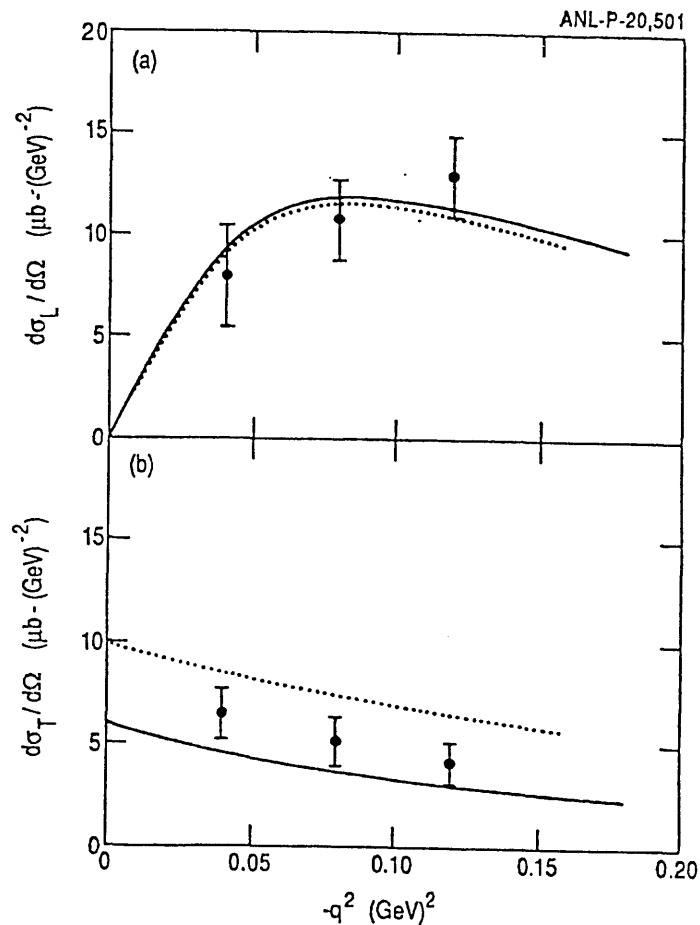


Fig. 12. The longitudinal ( $\sigma_L$ ) and transverse ( $\sigma_t$ ) cross sections of  $p(e,e'\pi^0)$  for the kinematics of Ref. 20. The dotted curves are obtained by setting the  $\Delta$  term to zero.

Saclay<sup>20</sup>. We see that both the  $\Delta$  term and the Born term are important in determining the transverse component of the cross section. However, the longitudinal part is completely dominated by the Born term. It was suggested in Ref. 20 that by choosing kinematics that  $\pi^0$  is in the direction of the virtual photon, the longitudinal cross section is dominated by the pion-exchange term, and hence it can be used to determine the pion form factor. This, however, is a very model-dependent statement. Within our model, the pion-pole term does not dominate the cross section at all angles, as illustrated in Fig. 14.

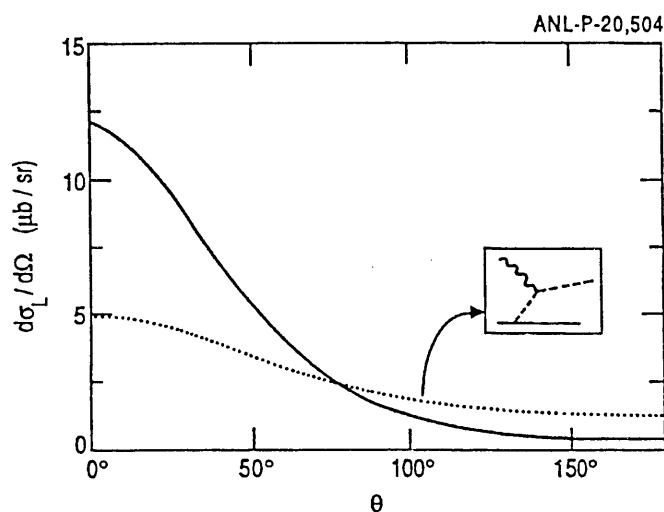


Fig. 13. Longitudinal cross section of  $p(e,e'\pi^0)$  for the kinematics of Ref. 20.

Only very limited progress has been made in applying the model to study reactions on nuclei. At the present time, we just finished the study of the  $d(e,e'\pi^+)$  reaction. Our results are compared with the data<sup>21</sup> in Fig. 14. We see that the predicted shape and magnitudes are in excellent agreement with the data. However, the position of the plate is about 5 MeV off the data. The reason is unclear at this time. The most difficult part of this calculation is the final nn scattering. This is done by using the

$\pi$ NN model developed<sup>22</sup> at Argonne. In Fig. 15, we show that the nn final-state interaction then can give significant contribution to the  $d(e,e'\pi^+p)$  cross section.

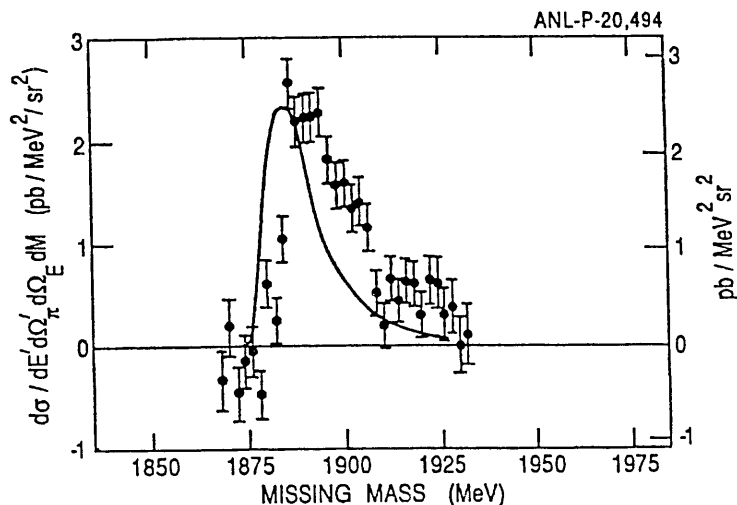


Fig. 14. Cross sections of  $d(e,e'\pi^+)$  are compared with the data of Ref. 21.

Our calculations of  $d(e,e'\pi)$  is the first step toward the application of our model to investigate nuclear dynamics. We are forming a collaboration to apply the model to study  ${}^3\text{He}(e,e'\pi)$  and  $A(e,e'NN)$ . Both involved large-scale calculations, and it will take us some time to obtain results for these complicated coincidences kinematics.

To end my talk, I would like to say that the theoretical effort, in particular the manpower, needed to explore new physics from the forthcoming precision data is currently very thin. Any rigorous calculations of the processes involving multi-particle final-states and/or polarizations are beyond the capability of a single person or even a group of two or three people. It is exciting to see new facilities, such as NIKHEF, Bates and CEBAF, will soon provide us with new data; but the data will serve no purpose unless the funding agencies start now to build the needed theoretical effort.

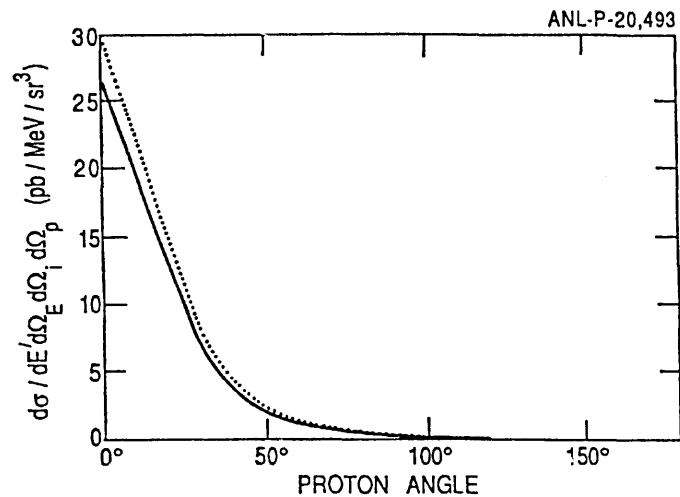


Fig. 15. Cross section of  $d(e,e'\pi^+n)$ . The dotted curve is obtained when the final  $nn$  interaction is neglected.

This work is supported by the U. S. Department of Energy, Nuclear Physics Division, under contract W-31-109-ENG-38.

#### REFERENCES

1. G. F. Chew, M. L. Goldberger, F. E. Low and Y. Nambu, Phys. Rev. **106**, 1345 (1957).
2. S. Fubini, Y. Nambu, V. Wataghlin, Phys. Rev. **111**, 329 (1958).
3. A. Donnachie, in High Energy Physics, ed. E. Burhop, vol. 5, (Academic Press, New York, 1972) p. 1.
4. M. G. Olsson and E. T. Osypowski, Nucl. Phys. **B87**, 399 (1975); Phys. Rev. **D17**, 174 (1978).
5. R. Wittman, R. Davidson and N. C. Mukhopadhyay, Phys. Lett. **B142**, 336 (1984).
6. J. L. Sabutis, Phys. Rev. C **27**, 778 (1983).
7. I. Blomquist and J. M. Laget, Nucl. Phys. **A280**, 405 (1977).

8. As reviewed recently by H. Gacilargo and T. Mizutani,  $\pi$ NN Systems, (World Scientific, Singapore, 1990).
9. A. W. Thomas, Advances in Nuclear Physics, eds. J. W. Negele and E. Vogt, vol. 13 (Plenum, New York, 1984) p. 1 and references therein.
10. H. Tanabe and K. Ohta, Phys. Rev. C **31**, 1876 (1985).
11. S. N. Yang, J. of Phys. **G11**, L205 (1985).
12. M. Araki and I. R. Afnan, Phys. Rev. C **36**, 250 (1987).
13. S. Nozawa, B. Blankleider and T.-S. H. Lee, Nucl. Phys. **A513**, 459 (1990).
14. S. Nozawa and T.-S. H. Lee, Nucl. Phys. **A513**, 511 (1990); **A513**, 543 (1990).
15. H. F. Jones and M. D. Scadron, Ann. of Phys. **81**, 1 (1973).
16. C. Lee, S. N. Yang and T.-S. H. Lee, J. Phys. **G17**, Nucl. Part. Phys. **17**, L131 (1991).
17. T.-S. H. Lee and B. Pearce, Nucl. Phys. **A530**, 532 (1991).
18. B. Pearce and B. Jennings, Nucl. Phys. **A528**, 655 (1991).
19. S. Nozawa, T.-S. H. Lee, B. Blankleider, Phys. Rev. C **41**, 213 (1990).
20. G. Bardin et al., Nucl. Phys. **B120**, 45 (1977).
21. R. Gilman et al., Phys. Rev. Lett. **64**, 622 (1990).
22. T.-S. H. Lee, Phys. Rev. Lett. **50**, 157 (1983); Phys. Rev. C **29**, 195 (1984).

**END**

---

**DATE  
FILMED  
2/20/92**

**I**

